Contribution of High-Resolution Correlative Imaging Techniques in the Study of the Liver Sieve in Three-Dimensions

FILIP BRAET,[1]* EDDIE WISSE,[1] PAUL BOMANS,[2] PETER FREDERIK,[2] WILLIE GEERTS,[3] ABRAHAM KOSTER,[4] LILIAN SOON,[1] AND SIMON RINGER[1]

[1]*Australian Key Centre for Microscopy and Microanalysis, The University of Sydney, New South Wales, Australia*
[2]*Electron Microscope Unit, Department of Pathology, University of Maastricht, Maastricht, The Netherlands*
[3]*Department of Molecular Cell Biology, Institute of Biomembranes, Utrecht University, Utrecht, The Netherlands*
[4]*Department of Molecular Cell Biology, Electron Microscopy, Leiden University Medical Center (LUMC), Leiden, The Netherlands*

KEY WORDS fenestrae; liver; whole mounts; vitrification robot; glove box; tomography

ABSTRACT Correlative microscopy has become increasingly important for the analysis of the structure, function, and dynamics of cells. This is largely due to the result of recent advances in light-, probe-, laser- and various electron microscopy techniques that facilitate three-dimensional studies. Furthermore, the improved understanding in the past decade of imaging cell compartments in the third dimension has resulted largely from the availability of powerful computers, fast high-resolution CCD cameras, specifically developed imaging analysis software, and various probes designed for labeling living and or fixed cells. In this paper, we review different correlative high-resolution imaging methodologies and how these microscopy techniques facilitated the accumulation of new insights in the morpho-functional and structural organization of the hepatic sieve. Various aspects of hepatic endothelial fenestrae regarding their structure, origin, dynamics, and formation will be explored throughout this paper by comparing the results of confocal laser scanning-, correlative fluorescence and scanning electron-, atomic force-, and whole-mount electron microscopy. Furthermore, the recent advances of vitrifying cells with the vitrobot in combination with the glove box for the preparation of cells for cryo-electron microscopic investigation will be discussed. Finally, the first transmission electron tomography data of the liver sieve in three-dimensions are presented. The obtained data unambiguously show the involvement of special domains in the de novo formation and disappearance of hepatic fenestrae, and focuses future research into the (supra)molecular structure of the fenestrae-forming center, defenestration center and fenestrae-, and sieve plate cytoskeleton ring by using advanced cryo-electron tomography. *Microsc. Res. Tech. 70:230–242, 2007.*

INTRODUCTION

Correlative microscopy (Robinson, 2001a), by using combined light-, probe-, laser-, and various electron microscope techniques, has become increasingly important for the analysis of the structure and function of cells and tissues. Correlative microscopy has witnessed a profound renaissance in the past years. New concepts and progress in cell biology have been discovered, thanks to improving correlative microscopy techniques, which continues to rely predominantly on advances in new, three-dimensional visualization techniques (Tsien RY, 2003). Ideally, correlative microscopy can be defined as an imaging platform aiming to capture exactly the same structures with multiple microscopy techniques on the same cell(s). Assuming that different microscopes provide different results, it is the special purpose of correlative microscopy to accumulate the related evidence preferably within one or more images. Such a combination of two or more different microscopy techniques, preferably with different resolution limits, can be referred to as correlative microscopy (Robinson, 2001a; Tsien, 2003). However, some microscopy techniques might be exempted from the above criteria, for example, the family of scanning probe microscopies, as they are able to gather simultaneously correlative topology and submembranous data on the same cell (Lillehei and Bottomley, 2000).

Correlative microscope methods have now become necessary technologies because of the need to bridge the gap between routine microscopy methods and three-dimensional reconstructions from micrometre to nanometre scale. The successful application of correlative microscopy and accompanying three-dimensional reconstruction is mainly ascribed to recent advances and availability of powerful computers, fast high-resolution CCD cameras, improved image processing software, and various probes specifically designed for

*Correspondence to: Filip Braet, Australian Key Centre for Microscopy and Microanalysis, Electron Microscope Unit, Madsen Building F09, University of Sydney, Sydney, NSW 2006, Australia. E-mail: filip.braet@emu.usyd.edu.au

Received 1 March 2005; accepted in revised form 1 May 2006

Contract grant sponsor: AKCMM; Contract grant sponsor: ARC/NHMRC FABLS Research Network Grant; Contract grant number: RN0460002; Contract grant sponsor: University Maastricht; Contract grant number: UM 131608; Contract grant sponsor: European 3D-EM Network of Excellence; Contract grant number: LSHG-CT-2004-502828.

DOI 10.1002/jemt.20408

Published online 5 February 2007 in Wiley InterScience (www.interscience.wiley.com).

labeling fixed and or living cells (Mironov et al., 2000). Corrrelative imaging allows the microscopist to gain additional morphological information and this provides a degree of confidence about the structures of interest as information obtained with one method can be compared to that seen with the other methods (Baldassarre et al. 2003; Robinson et al. 2001b; Svitkina and Borisy, 1999; Takizawa and Robinson, 2003). Furthermore, there is growing evidence from the literature that this approach of correlative imaging, preferably in multidimensions, facilitates the understanding of cellular and/or rare events by providing the possibility to collect new qualitative and quantitative information in a large sample volume (Grabenbauer et al., 2005; Takizawa and Robinson, 2006). Accordingly, this paper aims to provide an overview of different cutting-edge correlative high-resolution imaging methodologies, and how these microscopy- and image analysis techniques revealed new correlative insights into the hepatic endothelial fenestrae in three-dimensions (Braet, 2004a).

Hepatic endothelial fenestrae are dynamic structures that act as a sieving barrier to control the extensive exchange of material between the blood and the liver parenchyma. These membrane-bound pores lack a diaphragm and a basal lamina is also absent (Wisse, 1970), in contrast to fenestrae described in the kidney, pancreas, and brain (Braet and Soon, 2005). Their biological relevance in various diseases has been widely acknowledged (Braet and Wisse, 2002a; Fraser et al., 1995; Wisse et al., 1985).

CORRELATIVE FLUORESCENCE AND SCANNING ELECTRON MICROSCOPY

Many advances in the elucidation of structure-function relationships have relied upon fluorescence labeling (Mironov, 2000; Takizawa and Robinson, 2003). Correlative microscopy in which a fluorescence signal is reconciled with a signal from the electron microscope is an additional tool that can provide powerful information for cellular analysis (Robinson et al., 2001b; Tsien, 2003).

Fenestrae in vitro have a critical dimension in the order of 200 nm (Braet et al., 1994), making it necessary to use high-resolution microscopes, other than light microscopes to visualize these structures. Therefore, to correlate immunofluorescently labeled structures by confocal laser scanning microscopy with surface information at the electron-microscopical level, we developed a reproducible method to combine one fluorescent and one electron microscopic image of the same cell (Braet et al., 2002b), enabling us to obtain a snapshot of the morpho-functional relationships between the cytoskeleton and fenestrae (Fig. 1). In this method hepatic endothelial cells cultured on collagen-coated CELLocate-microgrid® glass cover slips were stained with rhodamine-phalloidin to visualize filamentous actin, and subsequently digital fluorescent images were then taken and cells located simultaneously by using the alphanumerical marked grids on the cover slip. In the next step, cover slips were recovered and further processed for scanning electron microscopy (Braet et al., 1997a). Previously visualized cells in the confocal laser scanning microscope were relocated with the aid of the alphanumerically marks and digital scanning electron micrographs of the corresponding cells were taken at an identical photographic end magnification. For correlative image analysis, the obtained data files were transferred to Adobe Photoshop Software or ImageJ (http://rsb.info.nih.gov/ij/) for color adjustment and figure assembly by using the replace color, leveling, and duplicate layer/merge options.

By using this correlative fluorescence- and scanning electron microscopy technique we could clearly illustrate a structural relation between filamentous actin and the surface topology of hepatic endothelial cells. Projecting the false color scanning electron micrograph on top of the corresponding actin stained cell revealed that filamentous actin was devoided inside the fenestrated areas. This was an important observation as it was believed that the pore-free microdomains in the middle of the fenestrated areas of microfilament-disrupted hepatic endothelial cells was composed of filamentous actin. Furthermore, the merged image data taught us that the brightly stained cytoplasmic actin dots matches with the fine globular topographic elevations present on the thin nonfenestrated arms, which divide the cytoplasm in sieve plates, and may consequently represent anchor sites for linking filamentous actin with the plasma membrane.

ATOMIC FORCE MICROSCOPY

The atomic force microscope is able to collect simultaneously correlative topology and submembranous structures on the same cell at high resolution (Braet and Wisse, 2004b). Sample deformation is believed to be an important component of the contrast mechanism in the visualization of living cells by atomic force microscopy, and originates from local variations in stiffness when the tip palpates the cell membrane (Radmacher, 2002). The cell stiffness or elasticity is mainly determined by the various organelles lying in the cytoplasm of the cell, and high-resolution imaging of submembranous cell compartments in the past was only possible when cells underwent detergent-extraction, fixation, and/or immunocytochemical staining, therefore precluding dynamic studies. As a consequence, indirect atomic force imaging of organelles, because the cell membrane is between the tip and the submembranous cell components, is a powerful tool to study organelle dynamics in intact living cells without the necessity of further preparative steps. Additionally, correlative topology data can be obtained simultaneously when fixation is applied, which increases the rigidity or stiffness of cells, resulting in images entirely dominated by surface details (Radmacher, 2002). The recent integration of atomic force- and confocal fluorescence microscopy in one instrument, combining the high-resolution topographical imaging of probe microscopy with the reliable biomolecular identification capabilities of optical microscopy is an interesting development (Kassies et al., 2005).

Atomic force microscopy has proven to be successful in hepatic endothelial cell imaging, by comparing atomic force images of fixed cells (Fig. 2A) with scanning- or transmission electron micrographs (Braet et al., 1996; Braet et al., 1997b). However, in the case of living hepatic endothelial cells, fenestrae as known by electron microscope studies could not be imaged (Fig. 2B), although small surface indentations could be visualized, suggesting the presence of fenestrae-like

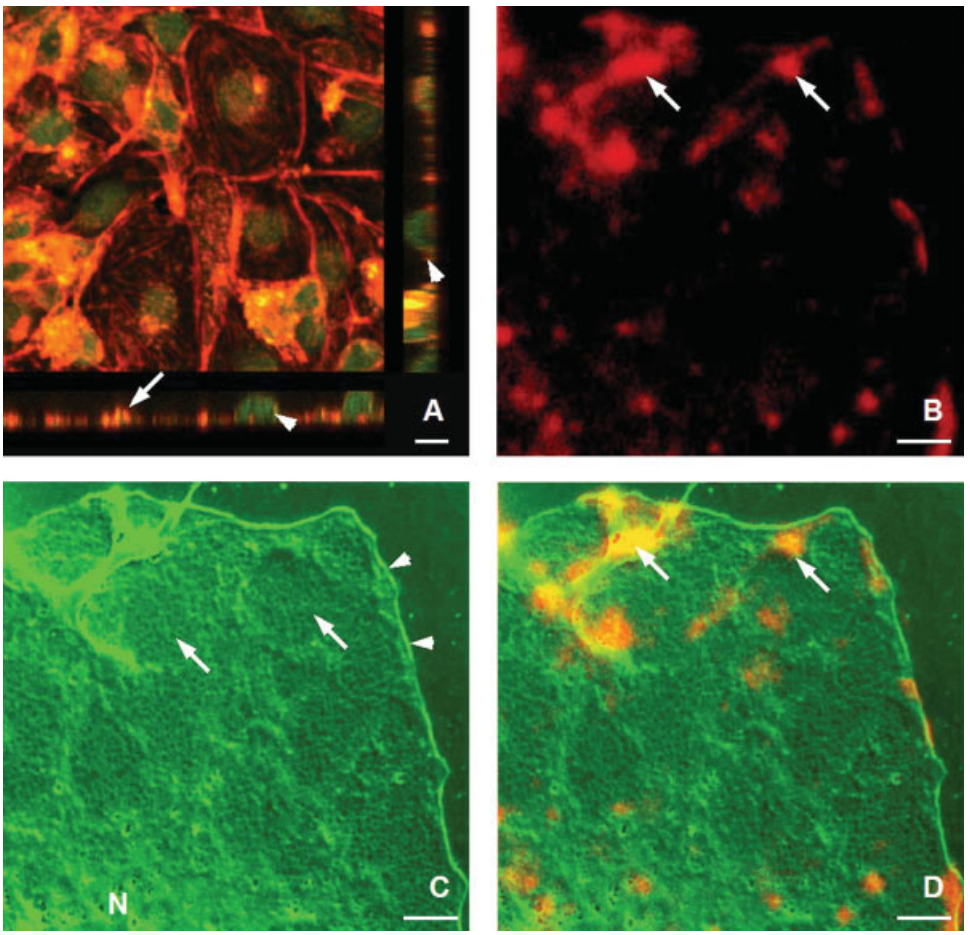

Fig. 1. Correlative confocal laser scanning (**A**,**B**), and SEM (**C**) micrographs of microfilament-disrupted hepatic endothelial cells. (**A**) Confocal laser scanning micrograph showing actin organization, monitored with rhodamine-phalloidin (filamentous actin/red) and fluorescein-DNase I staining (globular actin/green). The height images XZ (below) and YZ (right) reveal that filamentous actin is organized in patches along the thickness of the cell (arrow) and globular actin fluorescence (arrowhead) is mainly located around the perinuclear region. Scale bar, 5 μm. (**B**-**D**) Figure set shows simultaneous localization of fluorescent labeled filamentous actin (red) (**B**) in combination with topographic SEM information (green) (**C**) and the merged image information (**D**) of the same cell. High-magnification confocal laser scanning image **B** shows filamentous actin features similar as those seen in A: that is, brightly stained cytoplasmatic filamentous actin patches. Image **C** shows a green colored scanning electron micrograph of the fenestrated cytoplasm containing the sieve plates (arrows); cytoplasmatic border (arrowheads). The merge image **D** illustrates that the brightly stained filamentous actin dots matches with the fine globular topographic elevations present on the thin nonfenestrated cytoplasmic arms and that the sieve plates are devoid of filamentous actin; illustrating the additional value of applying different imaging techniques on the same cell. N, Nucleus. Scale bar, 2 μm.

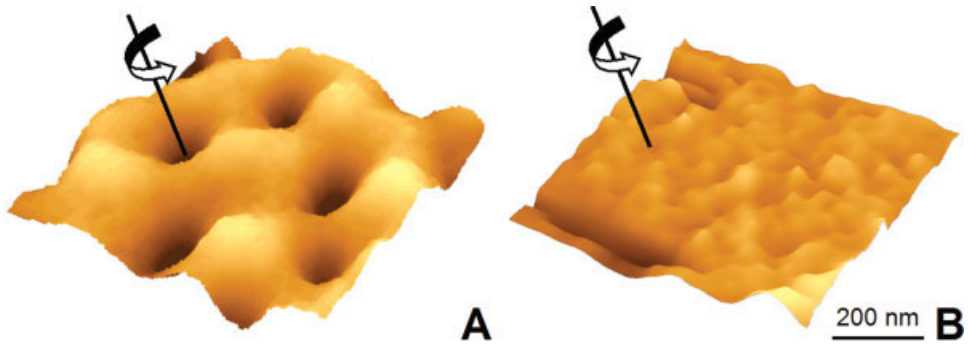

Fig. 2. Atomic force microscopy. High-magnification three-dimensional images showing the fenestrated cytoplasm of hepatic endothelial cells of glutaraldehyde-fixed (**A**) and living (**B**) cells obtained in contact mode at a loading force of 380 pN. (**A**) Wet-fixed cells reveal fenestrae (line arrow), as known by correlative SEM studies (see Fig. 1C). These open pores have an average diameter in undried conditions of 223 ± 44 nm, which is significant higher than the values obtained in dried-coated, or plastic embedded specimens. Height measurements reveal an average Z-value of 183 ± 48 nm. (n = 120). (**B**) Small surface indentations (line arrow) could be visualized when imaging living hepatic endothelial cells, suggesting the presence of fenestrae or pores (compare with A for the difference). These small features have a maximum diameter of 98 ± 52 nm and a Z-value of 92 ± 47 nm (n = 120), closely resembling the dimensions of coated-pits. Scale bar, 200 nm.

pores. The observed indentations have a maximum diameter of 98 ± 52 nm and a Z-value of 92 ± 47 nm, closely resembling the dimensions of coated-pits. Notably, by imaging the same cell before and after fixation, fenestrae with an average diameter of about 223 nm could be picked up easily in the fixed and undried state; although it was not possible to observe them in the living condition (Braet et al., 1998a). It was believed until recently that this was mainly due to the resolution limits of the microscope since the expected optimum resolution for a minimum loading force of 500 pN is 300 nm if the sample softness is 1 kPa (Braet et al., 1998a; Radmacher, 2002). Given that the living hepatic endothelial cell has an average elastic modulus of around 1 kPa, it was understandable that fenestrae could not be detected, which have a size of about 223 nm. However, the data presented in Figure 2B were recently obtained as a result of recent improvements in instrumentation using a loading force of 380 pN, resulting in an estimated resolution of about 180 nm.

From these correlative in vitro atomic force microscopy experiments, it became clear that fenestrae are difficult to image under certain conditions, which raised questions about the life span of fenestrae. The obtained atomic force microscope data on live cells are most probably indicating that fenestrae are continuously forming and disappearing in a small fraction of a time. In addition, this may also explain, together with the resolution limitations of the instrument (Braet et al., 1998a) and the damaging tip-sample interactions occurring during scanning (Braet et al., 2001a), why it was difficult to pick up fenestrae as known in the fixed and static state (Braet et al., 1997b). Without such a hypothesis, it is difficult to understand how such a porous hepatic endothelial lining in vivo is so resistant to the local blood pressure and the shear forces resulting from continuous friction with blood cells, in particular white blood cells (Wisse et al., 1985). Supplementary evidence for this hypothesis was found by the recent correlative cryo-electron microscopy observations in which we occasionally observed hepatic endothelial cells that were less fenestrated (see cryo-electron microscopy section). It was postulated that this was mainly due to the new physical fixation method applied, which takes place within milliseconds. This vitrification window may go along with the life span of fenestrae (Braet et al., 2004a). It is known that cryo-electron microscopy of rapidly frozen vitreous biological samples reveals the native structures of cells with details that differ considerably from those seen in conventional resin-embedded cells (Al-Amoudi et al., 2004). Therefore, correlating these atomic force- and cryo-electron microscopy data provided us with more evidence about the dynamic versus static nature of these pores, and may negate the alternate concept that fenestrae are a stationary type of open pores or channels.

CORRELATIVE TRANSMISSION ELECTRON MICROSCOPY OF SECTIONED VERSUS WHOLE-MOUNTED CELLS

Ultrathin Sectioning

The hepatic sinusoid and the endothelial lining have been studied mostly by transmission electron microscopy (TEM) rather than scanning electron microscopy. One reason for this was the earlier introduction of TEM, which was developed as a mainstream technique in biomedical research in the early sixties, whereas we had to wait for the application of scanning electron microscopy until the second half of the seventies. In contrast to some other microscopy approaches, one of the characteristics of transmission and scanning electron microscopy studies is the unpopular, laborious and time consuming preparation of the specimens. Meticulous processing of specimens in numerous steps in a complicated and semimagic procedure is crucial in high-resolution imaging of biological samples. Some steps are critical for the preservation of liver tissue, such as the initial perfusion fixation of the organ with glutaraldehyde (Wisse, 1970); others are less critical such as the storage of tissue in 70% alcohol. As a result, it is difficult for an inexperienced microscopist to adapt the complex preparatory procedure to the needs of a typical experiment at hand. Anesthesia, surgical skills, route of perfusion, gravity or pump perfusion, pressure, flow, composition, and sequence of perfusion fluids, saline washing, osmotic value, ion composition, quality of chemicals, prelevation techniques, cutting or fracturing of the tissue, the way and time intervals of changing fluids, temperature, and so on, they all play a role. Obviously, the quality of the final product follows from the quality of the preparatory process, but the possibilities for a professional approach to quality control are limited and often ambiguous. The evaluation of the quality of the specimen also regards the esthetics and therefore involves a touch of personal taste. Finally, the quality of the digital image on the screen and the printing of photographs are also involved. Besides, the reproducibility and the presence of a number of details in the specimen help to objectivate the evaluation.

Correlative microscopy however might help to find the way through a seemingly endless series of artifacts, accidents, and pitfalls. In the case of hepatic endothelial fenestrae it was essential to compare perfusion-fixed, plastic-embedded tissue in the transmission electron microscope with the results of freeze etching of fresh, unfixed tissue (Wisse, 1970) and whole mounts of cultured, (unfixed) frozen hepatic endothelial cells (Frederik et al., 1997). It appeared that hepatic endothelial fenestrae are equally imaged by these three "static" imaging techniques, thereby reducing the chance that fenestrae are preparatory artifacts. However, recent atomic force microscopy and vitrification studies on living hepatic endothelial cells provided additional insights about the "dynamic" nature (i.e., short life span) of hepatic endothelial fenestrae (see, corresponding sections). Anyway, perfusion fixation proved to be essential in TEM studies of fenestrae in ultrathin sections, because fenestrae simply disappear during immersion fixation, irrespective of double fixation (i.e., glutaraldehyde followed by osmium) or single osmium fixation (Wisse, 1970; Wisse et al., 1985).

In TEM sections (Wisse, 1970), the sinusoids are lined by three endothelial cell components: the perikaryon of the endothelial cell, cytoplasmic processes and sieve plates (Fig. 3A). The perikaryon contains the bulging nucleus and a standard set of organelles, such as the Golgi-apparatus, endoplasmatic reticulum, ribosomes, mitochondria, vacuoles, lysosomes, centrioles, and a multitude of small uncoated vesicles or vesicles

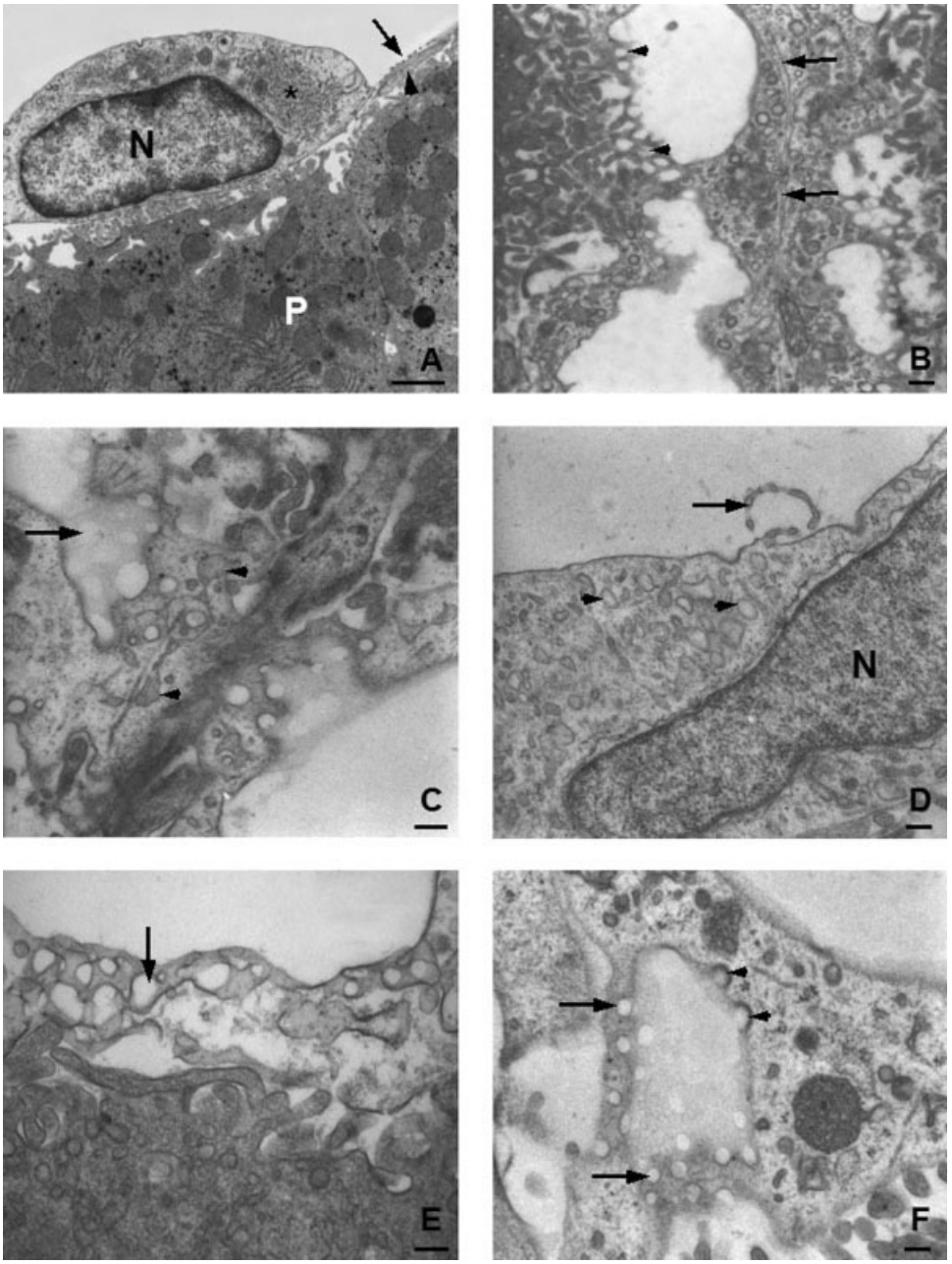

Fig. 3. TEM on sectioned rat, mouse and rabbit hepatic endothelial cells in situ. (**A**) Overview of an endothelial cell in a hepatic sinusoid of the rat. A bulging nucleus (N) is surrounded by cytoplasm containing numerous vesicles related to pinocytosis or to the Golgi-apparatus. To the right, a tubular network (*), probably a variant of the endoplasmic reticulum, connected to rough endoplasmic reticulum. Note, a connection to a sieve plate (arrow) is observed with an underlying process of a fat-storing (stellate) cell (arrowhead) in the space of Disse, which also contains numerous microvilli of the parenchymal cell (P). Scale bar, 1 μm. (**B**) Obliquely cut sieve plate and cytoplasm of a hepatic endothelial cell in mouse liver showing fenestrae (arrowhead) surrounded by organelle-free, filamentous dense cytoplasm. In the cytoplasm connected to the sieve plates, microtubuli (arrow) and many vesicles of different nature can be observed. Scale bar, 200 nm. (**C**) Obliquely cut sieve plate in a rabbit liver at higher magnification shows fenestrae (arrow) and in the cytoplasm, next to the sieve plate, one observes irregularly shaped saccules and branching tubular extensions of smooth endoplasmic reticulum (arrowhead). There is an apparent topographical relationship between this type of smooth endoplasmic reticulum and the periphery of sieve plates. Scale bar, 200 nm. (**D**) Higher magnification of a hepatic endothelial cell in rabbit liver, showing the structure of a loop (arrow). The loop consists of a circular sieve plate, containing fenestrae and the organelle-free, filamentous dense cytoplasm cut transversely in this section. Note, nucleus (N) vesicles (arrowhead). These loops probably relate to the defenestration centers seen in vitro. Scale bar, 200 nm. (**E**) Higher magnification of a small part of endothelial cytoplasm in rabbit liver, showing a complex structure consisting of fenestrae in a three-dimensional labyrinth (arrow). Comparable structures are seen when endothelial cells are isolated from the liver and internalize their sieve plates. The precise nature of these labyrinths is difficult to unravel in single ultrathin sections. Scale bar, 200 nm. (**F**) Coated pits (arrowhead) and fenestrae (arrow) have about the same size (rabbit liver). Coated pits pinch off from the cell membrane and are supposed to fuse with early endosomes after loosing their clathrin coating. Two-sided re-fusion with the opposing cell membranes of thin cytoplasmic processes might result in fenestrae formation. This type of imaging (i.e., static), however, does not provide further supporting evidence for a role of coated pits in fenestrae formation, other than the fact that the two structures are sometimes topographically close. Scale bar, 200 nm.

with bristle coating, pinching off from the cell membrane or smaller ones from the Golgi-apparatus. The perikaryon can be directly connected to sieve plates or can send out arms of cytoplasm that contain a limited set of organelles such as mitochondria, vacuoles, lysosomes, endoplasmatic reticulum, and vesicles. In both parts of the cell, straight microtubuli and groups of microfilaments are seen. Microtubules are seen to approach sieve plates (Fig. 3B), but from ultrathin sections it can not be concluded whether they surround the sieve plates, as is clearly seen as sieve plate associated cytoskeleton ring in whole mount preparations observed by transmission and scanning electron microscopy (see "whole mount TEM"-section). Sieve plates contain groups of fenestrae and are interspersed between cytoplasmic processes. Within the sieve plate, an electron dense filamentous network of material can be observed, enveloped between the two limiting cell membranes, a space which is devoid of all other small organelles, even ribosomes or other elements of the cytoskeleton. Therefore, the cytoplasm of the sieve plate only displays its filamentous ground substance.

Interestingly, the new findings obtained by studying TEM sections did not come to an end; although the ultrastructure of the hepatic sinusoidal endothelium is numerous times depicted since the first description of hepatic endothelial fenestrae in 1970 (Wisse, 1970). In a recent study on rabbit liver a few new structures could be found (Wisse, 2005; unpublished data) in addition to the ones described in earlier TEM studies using sectioned rat hepatic tissue (Wisse, 1970; Wisse, 1972; Wisse et al., 1985). First, close to the sieve plates we observe a saccular endoplasmatic reticulum, sometimes associated with a few ribosomes and often connected to tubular projections (Fig. 3C). This irregular membrane bound structure is observed in oblique sections through the endothelial lining. Second, a structure that we call a "loop" is found, consisting of a closed circle of bended sieve plate. We could only correlate this structure with the so-called defenestration center found in hepatic endothelial cells treated in vitro with antimycin A (Braet et al., 2003b). These loops found in vivo, however, seem to be comparable in structure but larger than the defenestration center observed in vitro (Fig. 3D). Incidentally, we observe complexes of intracytoplasmic fenestrae, as are also seen during isolation of rat hepatic endothelial cells. These labyrinth-like structures display a high degree of complexity (Fig. 3E). In addition, we sometimes observe longer transendothelial channels other than fenestrae, but their frequency is very limited in TEM studies using sections; and consequently, electron tomography modeling may provide us with additional ultrastructural information regarding these peculiar structures. Furthermore, the fact that hepatic endothelial cells are highly endocytotic cells is reflected by the presence of bristle-coated micropinocytotic vesicles, which pinch off all over the luminal surface of hepatic endothelial cells and their processes. Only very few vesicles can be seen to pinch off at the abluminal surface of the cells. Coated pits can also be seen both in scanning electron microscopy, but their frequency seems to be low, most probably due to the fact that visualization by scanning electron microscopy is restricted to the very early stages of pinching off of coated pits. Sometimes they are close to the sieve plates and it is tempting to assume a relation-ship in fenestrae formation (Fig 3F). Coated pits have the right size to form fenestrae when they would fuse with the two opposite cell membranes (*vide infra*).

Noteworthy, scanning electron microscopy preparations provide a direct overview of the endothelial surface, which is an advantage for the observer to orient him/herself when studying the liver tissue, and therefore seem to be ideal for counting and measuring of fenestrae per unit surface area (Braet et al., 2001b). However, scanning electron microscopy preparations are subject to shrinkage in the order of 30% and this condition seems to exclude accurate measurements on fenestrae in situ unless a well-calculated correction factor for shrinkage is included in the process (Braet et al., 1994; Braet et al., 1997a; Wisse et al., 1985). An additional problem is put forward by sputter coating, needed to give electrical conductivity to the specimen surface. This also narrows the fenestrae by precipitating a thin layer of heavy metal on top of the specimen and the margin of fenestrae (Braet et al., 1996). Therefore, for exact measurements of the diameter of fenestrae in situ, TEM studies are at current the only recommended approach, since plastic embedding preserves the tissue from shrinkage (Wisse et al., 1985). This implies finding places in ultrathin sections where sieve plates are obliquely cut and where fenestrae show up with part of the sieve plate included (Fig. 3B). By using this approach a significant difference in diameter between periportal and centrolobular fenestrae was measured in rats (175 versus 147 nm, respectively) (Wisse et al., 1985), together with a significant difference between rat and rabbit fenestrae (rabbit 108 nm) (Lievens et al., 2004). Although differences in diameter and number of fenestrae exist among different species, the ultrastructure of hepatic endothelial fenestrae is the same across species (Braet and Wisse, 2002a).

Whole Mounts

One of the most straightforward ways to observe the overall complex organization of the cytoskeleton at high resolution is to examine whole mounts of cells by TEM (Lindroth et al., 1992). This technique allows the visualization of the cytoskeleton with minimal disruption of the cells after slight prefixation and brief extraction with detergent. If desirable the method can be combined with immunogold labeling (Bell et al., 1989). On the contrary, it is impossible to get a nice plane overview picture of the overall cytoskeleton of a cell on the basis of ultrathin TEM sections (i.e., 60 nm) as a result of technical limitations. These limitations include the extremely small portion of the total cell volume that is included in a section, the tendency of fine and thin structures cut obliquely or in cross section to disappear visually into the cytoplasmic ground substance, and also the small differences in contrast between some of these structures and the plastic embedding medium. Therefore, as outlined, we preferred whole mounts of hepatic endothelial cells grown on electron microscope supports (Fig. 4A) as a model system for high-resolution transmission electron microscope investigation of the cytoskeleton associated with fenestrae.

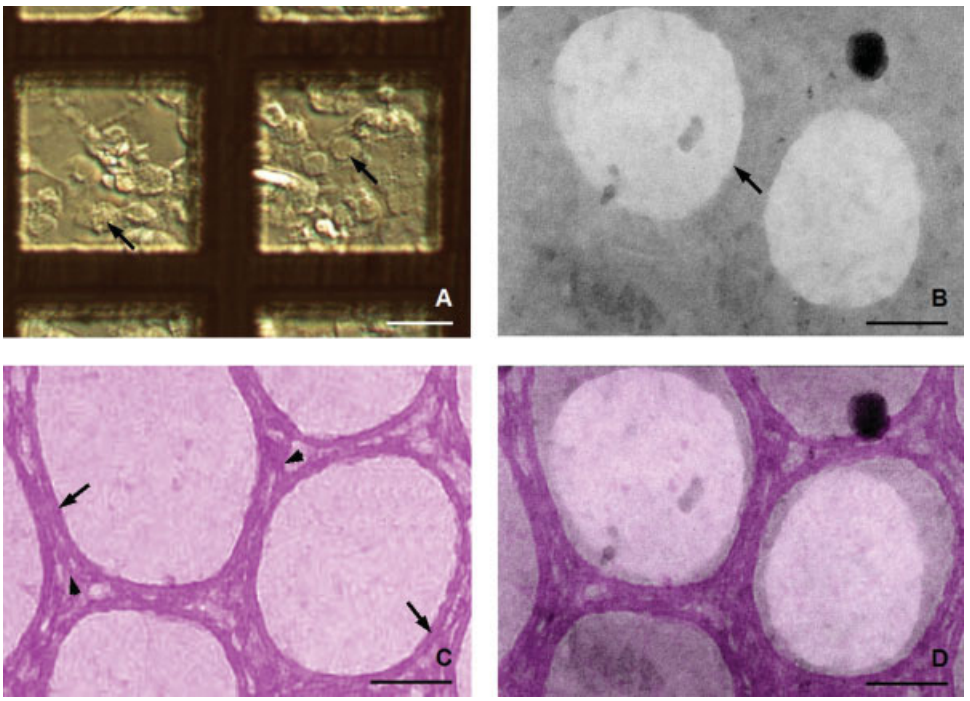

Fig. 4. Whole-mount TEM. (**A**) Light microscopic image of hepatic endothelial cells growing on 300-mesh nickel grids covered with a Formvar film and coated with soluble collagen. Scale bar 30 μm. (**B–D**) High-power transmission electron micrographs of a nonextracted (B); and of a formaldehyde prefixed, cytoskeleton buffer extracted hepatic endothelial cell (**C**). Notice the membrane-bound fenestrae (arrow) in micrograph **B**; and a remarkable series of rings of fenestrae-associated cytoskeleton in **C**. Note that the rings are connected to the fine branching cytoskeleton elements (arrowhead) surrounding the fenestrae. (**D**) Layering the purple colored transmission electron micrograph on top of the cell surface of a nonextracted hepatic endothelial cell clearly illustrates the architectural relation between both structures and the additional value of correlative image analysis. Scale bars, 100 nm.

In this method, hepatic endothelial cells were cultured on Formvar-coated (1%) nickel grids (300 mesh), later coated with diluted collagen solution (1:90). The cells were fixed with 4% formaldehyde in PBS for 1 min at 21°C followed by extraction with cytoskeleton stabilizing buffer for 1 min at 21°C (Braet et al., 1995). After extraction, cells were fixed as for scanning electron microscopy, and dehydrated in graded ethanol solutions and subsequently hexamethyldisilazane-dried (Braet et al., 1997a). For comparative purposes, it is advisable to include unextracted control samples in the experiment (Fig. 4B). These data can be used for comparative computational image analysis to gain additional insight into the extracted versus unextracted state (Fig. 4B–4D), providing a degree of confidence for the interpretation of detergent-extracted whole mount cells. Of note, the whole mount specimens can be examined in any type of transmission electron microscope at an accelerating voltage of 80–120 kV.

The results of these whole mount electron microscope studies on hepatic endothelial cells have added the following decisive insights in the ultrastructure of the cytoskeleton in fenestrated areas, (Figs. 4C and 4D) which could not be obtained in a convincing way when embedded and sectioned cells were used: (i) sieve plates and fenestrae are delineated by cytoskeleton elements; (ii) fenestrae are delineated by a filamentous, fenestrae-associated cytoskeleton ring with a mean filament thickness of 16 nm, (iii) sieve plates are surrounded by a ring-like orientation of microtubuli, which form a network together with additional branching cytoskeletal elements (Braet et al., 1995); and (iv) the fenestrae-associated cytoskeleton ring is always there, also when the number and size of fenestrae changes after different treatments (Braet et al., 1998b).

Obviously this whole mount approach is a potent microscopy tool for many areas of structural cell biology (Peachey et al., 1996), but is, as with every visualization method, characterized by its limitations. Rendering structural details to be found in the thicker parts of the cytoplasm for example can not be resolved in whole-mount electron microscopy due the mass thickness, resulting in electron dense images characterized by the lack of any fine structural detail. As a consequence, important phenomena may be overlooked visually and therefore, simultaneous correlative ultrathin sectioning is strongly recommended. In our work, the correlative study of sections and whole mounts was necessary to entirely characterize the structure responsible for fenestrae formation. The whole mount approach allowed us to pickup fenestrae-forming centers easily (Braet and Wisse, 2002a); whereas, tangentially and transversely sectioning revealed that the cytoplasm surrounding these centers contained thin filaments fanning out in the surrounding cytoplasm which could be not be seen in whole mounts (Braet et al., 2002b). These thin filaments seem to serve as an anchor for the fenestrae-forming centers within the middle of the sieve plates or serve as a guidance for the

newly formed fenestrae, which ebb away in the fenestrated areas. Together, whole-mount TEM can never replace the obvious advantages of investigating ultrathin TEM sections. Ideally, both methods should be used in combination as correlative transmission electron microscope imaging methods, harmonizing the advantages of both complementary techniques as presented in this section.

CRYO-ELECTRON MICROSCOPY

It is well known that chemical fixation, dehydration, and drying or embedding/sectioning of cells can induce image artifacts resulting in different observations when different preparation techniques are applied (King, 1991). To assess whether the observations on the fenestrae and the surrounding cytoskeleton are artifacts introduced by preparation procedures we initiated cryo-electron microscopy studies on whole mount hepatic endothelial cells cultured on electron microscopic grids. In cryo-electron microscopy, living cells are physically fixed by rapid cooling, enabling their study as whole mounts without the necessity of further preparation steps. However, TEM of thin cells in toto, such as hepatic endothelial cells or fibroblasts, has long been tried and considered impossible or extremely difficult because of the mass-thickness of the specimen. This view is usually substantiated by failures reported in the literature. Culturing cells as a single layer thick on grids, beam-specimen interaction resulting in specimen damage and also problems associated with cryo-specimen preparation have been held responsible for this failure depending on the spirit of the time. More than 10 years ago the possibilities of cryo-electron microscopy on whole-mounted hepatic endothelial cells was discussed. By that time, the isolation and culture of hepatic endothelial cells on electron microscopy grids became established (Braet et al., 1995) and cryo-electron microscopy became an accepted approach for cellular imaging as supported by the cryo-observations on intact blood platelets (Frederik et al., 1991a) and bacteria (Frederik et al., 1991b), revealing subcellular details such as organelles, membranous structures and cytoskeleton elements. It was argued, based on preliminary atomic force microscopy data (Braet et al., 1996), that the thickness of hepatic endothelial cells was of the same dimensional order as blood platelets and bacteria, and thus cryo-electron microscopy imaging could be expected using intermediate voltages. This holds especially for the thin fenestrated areas of cultured hepatic endothelial cells, which have a thickness of less than 100 nm, thus in the order of the thickness of thin films used in cryo-electron microscopy to visualize lipid nanoparticles and proteins (Templeton et al., 1997). As a result, electron beam-related problems (damage) or electron optical limitations were therefore not to be expected. The remaining challenging task was to find a correct and reproducible way for the preparation of vitrified cultured endothelial cells for cryo-electron microscopy investigation.

For cryo-electron microscopy sample preparation, a guillotine-like device (guided drop principle) used to be the standard approach in the early 1990s for fast vitrification of an electron microscopic grid in liquid ethane. The grid is held by forceps mounted to the guillotine and after manually blotting by the aid of filter paper, excess liquid is taken away leaving a thin aqueous specimen behind ready for vitrification by plunging into melting ethane sludge. Accordingly, the initial attempts to vitrify hepatic endothelial cells were done with an open air guillotine method in combination with a homemade version of the controlled environment vitrification system (Bellare et al., 1988). The results were for the most part disappointing because most of the aqueous area left behind on the electron microscopic grid was too thick for the electron bundle to penetrate, and in the few thin areas the hepatic endothelial cells looked severely distorted and damaged. We held improper blotting responsible for these failures, resulting in the loss of fenestrae, formation of artifactual gaps and lack of structural details in the cytoplasm (Frederik et al., 1997).

By that time we embarked on the development of an automated and computer-controlled vitrification system that ultimately culminated in the Vitrobot™ (patented by the University Maastricht http://www.maastrichtinstruments.nl/projects/VR/index.html, and licensed to F.E.I.). Automation of a reproducible blotting procedure appeared to be a key element for successful vitrification, and consequently a blotting mechanism was developed and tested thoroughly before considering further process control (Frederik et al., 2000). Interestingly, by eliminating variations in the blotting process, we became aware of the importance of controlling the environmental humidity (Frederik and Hubert, 2005) for the outcome of a cryo-preparation. Humidity has a 2-fold effect on the aqueous specimen; the temperature is lowered to the dew-point temperature and the temperature difference thus established results in a heat influx to the specimen that leads to further evaporation. Consequently, specimen temperature and osmolarity are thus controlled by the environmental humidity. The temperature will attain the dew point temperature within fractions of seconds (e.g., when an environment at 40°C and a relative humidity of 40% is assumed it takes 0.1 s for a 0.5-μm thick specimen and 0.8 s for a 5-μm thick specimen). As soon as the dew point is attained, evaporation will proceed at a rate of about 60 nm/s (evaporation from two-sides of the specimen in the same environment, 40°C and a relative humidity of 40%). During the manipulation of a wet electron microscopic grid in the air, the dew point temperature will be attained and depending on the amount and nature of fluid carried along with the grid, osmotic effects come into play. With micro-liters of water on the grid, the osmotic effect is small; a 3 μL drop on a grid represents a cylinder of 500 μm and the handling of such a grid for a few seconds evaporation at a rate of 60 nm/s will hardly affect the osmolarity. This situation changes when the specimen becomes thin, in the order of the thickness of the thin rims of a cultured cell, i.e., in the order of about 100 nm. Manipulation of the electron microscopic grid through the air will at this moment seriously affect the osmolarity since it can double in a second. This example is presented to give some indication of the time scales involved in temperature and osmotic changes that cultured cells may undergo during preparation for cryo-electron microscopy. Furthermore, this example explains and justifies the need for humidity control at near saturated levels (relative humidity more than

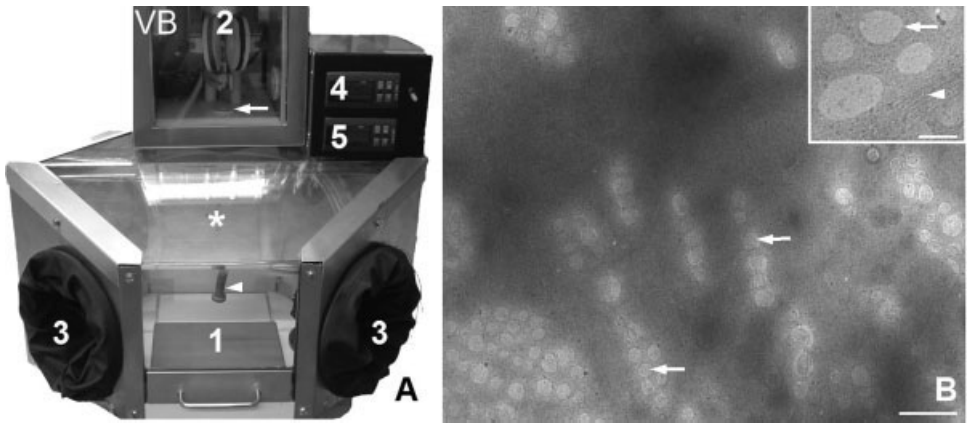

Fig. 5. Cryo-electron microscopy. (**A**) Photograph showing the glove box placed under the Vitrobot™ (VB). Note, only the lower part of the robot is shown. The culture dish containing the grids with cultured cells is placed on the work-platform (1) of the glove box via a drawer system. The grids are collected with a special tweezers equilibrated within the chamber, which can be mounted on the guiding rod of the vitrification robot (2). All manipulations are done through the glove ports (3) and with the aid of a local light source (arrowhead). Note the acrylic window with "glass-like" clarity in the glove box (*). Inside the glove box a Peltier type of heating/cooling element, an ultrasonic atomizer used for humidification of the working space, and an electronic sensor to monitor the humidity (4) and temperature (5) in the working space is present. After the mounting of a grid in the special forceps, the forceps with grid will be lifted automatically into the Vitrobot™. Upon closing a shutter (arrow) at the bottom plate of the vitrification robot, the glove box can be disconnected and a container with melting ethane is placed instead taking over the location of the glove box. Specimen processing in the Vitrobot™ and vitrification is fully computer-controlled. (**B**) Intermediate magnification image of a vitrified hydrated whole-mounted hepatic endothelial cell; obtained under controlled sample handling conditions by using a glove box in combination with the Vitrobot™ as described previously (Braet et al., 2003a), showing intact fenestrae (arrow) grouped in sieve plates. Scale bar, 400 nm. Inset shows a high magnification image of fenestrae and the associated cytoskeleton (arrow). Note the cytoskeleton elements (arrowhead) running alongside the fenestrae. Scale bar, 150 nm.

95%) during manipulation and preparation of a monolayer of cultured cells. Therefore, the osmotic vulnerability of a cell monolayer comes into play when excess water/buffer is removed to obtain an optimally thin specimen for vitrification and cryo-observation. This theoretical example is supported by our earlier cryo-electron microscopic observations in which hepatic endothelial cells still showed the presence of a small number of gaps probably due to the lack of proper handling procedures under environmental controlled conditions when transferring the electron microscopic grid to the vitrification robot (Braet et al., 2003a). At this stage, hepatic endothelial cells are only covered with a submicron layer of water and are consequently vulnerable to temperature effects and osmotic damage as discussed above. Therefore, the use of a temperature and humidity controlled glove box in conjunction with a Vitrobot™ (Fig. 5A) was found essential for the manipulation of hepatic endothelial cells from culture conditions towards the preparation for cryo-electron microscopy investigation (Braet et al., 2003a). A cryo-electron microscopic image of such a preparation is presented in Figure 5B. Fenestrae and the surrounding cytoskeleton elements and different membrane-bound organelles could be easily observed in these types of cryo-images without the presence of gaps, indicating that our earlier observations on the fenestrae-associated cytoskeleton is not an artifact introduced by chemical fixation, partial extraction or other preparation procedures (Braet et al., 2003a). Further improvements in cryo-imaging may be expected for the future when higher accelerating voltages are used (300 kV instead of 120 kV) in conjunction with electron tomography (*vide infra*).

From these cryo-experiments on hepatic endothelial cells, it became apparent that taking excess culture medium away under careful blotting conditions was an essential factor for the successful preparation of a monolayer of cells for cryo-electron microscopy studies (Frederik et al., 1997; Frederik et al., 2000). In addition, by gaining experience with automatic blotting we came to the conclusion that the control of environmental humidity during manipulation of vulnerable cells by using the Vitobot™ in combination with the glove box is the final key factor to successful preparation of cell monolayers for cryo-electron microscopy (Braet et al., 2003a). It can be expected when the time resolution of vitrification is fully exploited, in conjunction with spatial resolution, cryo-electron microscopy may significantly contribute to the ultrastructural study of membrane dynamics in model systems as well as in (intact) biological specimens. In any case, once a cell is vitrified correctly the challenge becomes to extract all the available three-dimensional information and in the time-domain (i.e., four-dimensional information). This fourth dimension may provide additional evidence about the dynamic versus static nature of fenestrae as discussed in the "Atomic Force Microscopy" section. The lag time of this overall conclusion is remarkable, but we think that the standardized cryo-sample preparation approach due to the recent development of hardware, such as the Vitrobot™ for reliable blotting and vitrification, will soon gain momentum. Finally, tomography at the cryo-electron microscopy level is able to resolve details at a three-dimensional resolution better than 3 nm in a specimen of 100 nm thick, providing a solid basis for tomography as an emerging three-dimensional technology that may greatly contribute to the three-dimensional

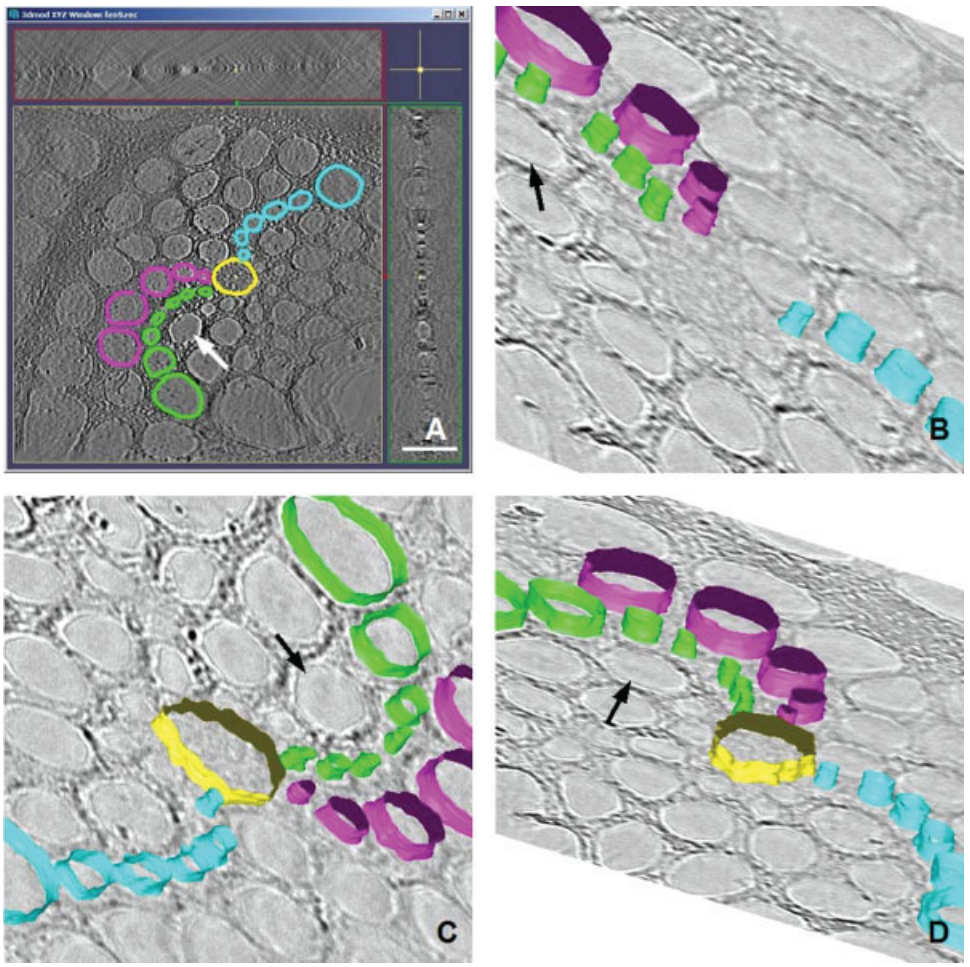

Fig. 6. Electron tomographic reconstruction of a fenestrae-forming center (yellow) and connected fenestrae (arrow) rows (row 1, green; row 2, purple; and row 3, blue) as observed in a whole mount formaldehyde prefixed, cytoskeleton buffer extracted hepatic endothelial cell. High-magnification digital images of the fenestrated areas of whole mount hepatic endothelial cells (1024 × 1024 pixels) were captured with a slow scan CCD camera (Temcam F214, TVIPS GmbH, Germany) in an angular range of typically −65 to +64° with 1° increment. The tilt series were recorded automatically using a dedicated single axis high tilt tomography holder in conjunction with the OpenTomo software package or Xplore3D (F.E.I. Company, The Netherlands). By means of the IMOD program package: the tilt series were aligned via fiducial markers (10 nm Ø gold beads); subsequently, the single-axis tilt tomograms were computed using resolution-weighted back projection and combined into one dual axis tilt tomogram; and finally, contouring models of the fenestrae-forming center were produced by computer-assisted tracking of high contrast lines and planes within the tomograms using IMOD. The tomograms had a final resolution of about 4 nm. Scale bar, 200 nm.

study of intact cells at the (supra-) molecular level as will be outlined in the next section.

ELECTRON TOMOGRAPHY

Although the basic concepts of electron tomography were already described in the early 1960s, during the last decade transmission electron tomography has become an important tool to obtain three-dimensional information on cellular structures within the resolution range of 3–10 nm. New technical aspects were needed to support the emerging method of three-dimensional electron microscopy tomography, such as very stable tilting stages, specific specimen holders for high tilt angles, sensitive large-scale CCD-cameras, automated data acquisition programs and software packages for the alignment, the reconstruction and the analysis of the recorded tilt images and tomograms became available both on a commercial and academic basis.

The procedure to obtain a tomogram (i.e., three-dimensional transmission electron microscopic reconstruction) of a specimen has been described extensively elsewhere (Frank et al., 2002; McEwen and Frank, 2001). Briefly, a series of images (projections) is recorded, usually from −65 till +65 degrees with an increment of 1° and the average time for recording a single tilt series takes less than an hour. The maximum allowable thickness of the specimen depends on the high-tension of the microscope and on the radiation sensitivity of the specimen (the allowable electron dose). Typically, with a 200 kV transmission electron microscope, a resin-embedded and stained section of ~250–300 nm in thickness can be imaged successfully. Sophisticated data acquisition software (Geerts et al., 2006) are available for transmission electron microscopes for recording large series of

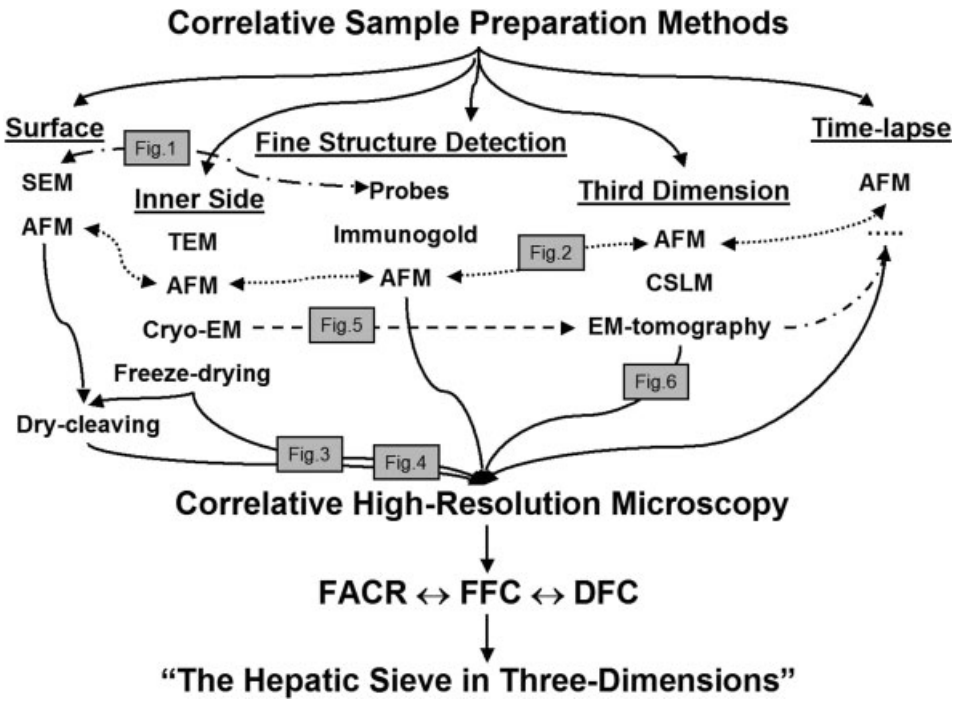

Fig. 7. Schematic diagram illustrating how the different correlative sample preparation methods applied on hepatic endothelial cells revealed new "correlative" insights into the study of the hepatic sieve in three-dimensions. Note the powerfull imaging capacibilities of atomic force microscopy, allowing to gain surface and submembranous three-dimensional ultrastructural information in living cells from the micrometre to nanometre scale. Though fenestrae are difficult to image with the AFM (Fig. 2), recent advances in the field of probe microscopy will probably allow visualization of fenestrae in living cells with less loading force. For the future it can be expected that cryo-electron microscopy (Fig. 5) combined with tomographic analysis (Fig. 6) will further contribute to understanding the molecular structure of fenestrae in the fully hydrated state. FACR, fenestrae-associated cytoskeleton ring (Braet et al., 1995); FFC, fenestrae-forming center (Braet et al., 1998b); DFC, Defenestration center (Braet et al., 2003b).

two-dimensional images, while tilting the specimen stage over as wide as possible angular ranges. Next, after data acquisition, the series of 131 images are accurately aligned making use of fiducial markers (usually gold particles) that were deposited on the surface or inside the specimen. The subsequent step, the 3D reconstruction, often referred to as the tomogram, is computed by an approach like the weighted back projection. The Z-resolution of the reconstruction depends on the angular tilt range and the tilt angle increments (determines the number of images), and on the section thickness. Because of mechanical/physical reasons of the transmission electron microscope specimen-holder the practically useable tilt range is limited. Often, image quality is absent or too poor beyond tilt-angles of -65 and $+65$ degrees. The missing projections—typically from -65 to -90 and from 65 till 90°—correspond to a missing wedge of information in Fourier space, and is referred to as the missing wedge. The visual effect of the missing wedge is that objects appear to be elongated and that the resolution in a tomogram is not the same in all directions in the tomogram (i.e., anisotropic resolution). The missing wedge can be significantly reduced by taking the grid out of the microscope, by rotating the grid 90°, inserting the grid again, relocating the area imaged during the first tilt series, and by recording a second tilt-series. The two reconstructions can then be combined and instead of a missing wedge we have a missing cone. The latter procedure is referred to as dual-axis electron tomography (Mastronarde, 1997; Penczek et al., 1995; Taylor et al., 1984). After generation of the tomogram the data will need to be analyzed by computer visualization techniques using dedicated techniques like volume rendering and modeling. For these purposes several commercial or academic software packages are available as outlined above.

Electron tomographic sectioning and subsequent three-dimensional reconstruction/modeling of the fenestrated cytoplasm of misakinolide-treated hepatic endothelial cells (Braet et al., 1998b) revealed the remarkable ultrathin dimensions of the fenestrae-forming center and connected fenestrae rows with increasing diameter (Fig. 6). Moreover, the three-dimensional reconstructions provided additional information that the thickness (Z-dimension) of the fenestrae-forming center and the rows of newly formed fenestrae fanning out into the surrounding fenestrated cytoplasm seems to be similar with the neighboring cytoskeleton elements and existing fenestrae. This became apparent when depicting the reconstructions under different angles (Figs. 6C and 6D). In view of that, these data seem to support our earlier assumptions in which we postulated that these (membrane-bound) centers and pores are most likely composed of a single layer of cytoskeleton elements interspersed/sandwiched between the cell membrane (Braet et al., 1995; Braet et al., 2001a).

Interesting is the cylindrical shape of the reconstructed fenestrae, which show in the middle a groove-

like indentation (Figs. 6B and 6C). This groove may correspond to the location of the fenestrae-associated cytoskeleton ring as observed in detergent-extracted whole mounts of hepatic endothelial cells (Fig. 4C). Furthermore, the modeling provided additional information that the fenestrae-formation centers show small indentations at the circumference comparable to the size of the smallest fenestrae connected to these gray centers (Fig. 6D). This probably indicates that the newly formed fenestrae are docking off from that point and that the rim of the fenestrae-forming centers may serve as a wharf when the newly formed pores ebb away in the surrounding fenestrated cytoplasm. Accordingly, this is an area to be fully explored and open up new research directions to define with the aid of immunogold labeling studies which molecules are involved in the formation of a single fenestra at the rim of a fenestrae-forming center by imaging vitrified hepatic endothelial cells with transmission electron tomography.

CONCLUDING REMARKS

Innovations in correlative imaging methods (Leapman, 2004) coupled with computational advances (Carrington and Lisin, 2004) have lately led to significant advances in the understanding of cell function and complex cellular systems (Afzelius and Maunsbach, 2004). In addition, ground-breaking developments in microscopy can be expected in this exciting era of digital technology and will certainly speed up scientific breakthrough on cellular nanostructures over a wide range of length and time scales. High-speed cameras, predictive computer models, new data-processing methods, multifunctional microscopes are a few examples which will undoubtedly boost the application of correlative microscopy imaging methods to the broader audience. Ideally, this technology will contribute directly to identifying and characterizing the complex molecular machinery of cells in three-dimensions.

From this paper it became clear that the application of different high-resolution correlative microscope methods during our fenestral studies in the hepatic endothelial cell model facilitated the accumulation of new insights in the morpho-functional and structural organization of the liver sieve (Fig. 7). The data obtained over the past 10 years unambiguously showed the involvement of special subcellular components in de novo formation and disappearance of fenestrae, and focuses future research into the three-dimensional supramolecular structure of the fenestrae-forming center (Braet et al., 1998b), defenestration center (Braet et al., 2003b), and sieve- and fenestrae-associated cytoskeleton ring (Braet et al., 1995) in the fully hydrated state by using computer-controlled physical fixation (Braet et al., 2003a) and state-of-the-art cryo-electron tomography in combination with correlative immunogold labeling (Frank et al., 2002; Grunewald et al., 2003; Koster and Klumperman, 2003).

ACKNOWLEDGMENTS

The authors acknowledge the facilities as well as scientific, technical and administrative assistance from staff in the NANO Major National Research Facility at the Electron Microscope Unit of the University of Sydney. With respect to Figure 6, the authors are grateful to Prof. Ilan Spector (State University of New York) for his expert assistance in performing the antiactin drug experiments.

REFERENCES

Afzelius BA, Maunsbach AB. 2004. Biological ultrastructure research; the first 50 years. Tissue Cell 36:83–94.

Al-Amoudi A, Norlen LP, Dubochet J. 2004. Cryo-electron microscopy of vitreous sections of native biological cells and tissues. J Struct Biol 148:131–135.

Baldassarre M, Pompeo A, Beznoussenko G, Castaldi C, Cortellino S, McNiven MA, Luini A, Buccione R. 2003. Dynamin participates in focal extracellular matrix degradation by invasive cells. Mol Biol Cell 14:1074–1084.

Bellare JR, Davis HT, Scriven LE, Talmon Y. 1988. Controlled environment vitrification system: An improved sample preparation technique. J Electron Microsc Tech 10:87–111.

Bell PB, Lindroth M, Frederiksson BA, Liu XD. 1989. Problems associated with preparations of whole mounts of cytoskeletons for high resolution electron microscopy. Scan Electron Microsc 3:117–135.

Braet F. 2004a. How molecular microscopy revealed new insights in the dynamics of hepatic endothelial fenestrae in the past decade. Liver Int 24:532–539.

Braet F, Soon LL. 2005. Diaphragmed fenestrae in the glomerular endothelium versus non-diaphragmed fenestrae in the hepatic endothelium. Kidney Int 68:1902–1903.

Braet F, Wisse E. 2002a. Structural and functional aspects of liver sinusoidal endothelial cell fenestrae: A review. Comp Hepatol 1:1.

Braet F, Wisse E. 2004b. Imaging surface and submembranous structures in living cells with the atomic force microscope: Notes and tricks. In: Braga PC, Ricci D, editors. Atomic force microscopy: Methods and protocols in biomedical applications. Totowa, NJ: Humana Press. pp. 201–216.

Braet F, De Zanger R, Sasaoki T, Baekeland M, Janssens P, Smedsrød B, Wisse E. 1994. Assessment of a method of isolation, purification and cultivation of rat liver sinusoidal endothelial cells. Lab Invest 70:944–952.

Braet F, De Zanger R, Baekeland M, Crabbé E, Van Der Smissen P, Wisse E. 1995. Structure and dynamics of the fenestrae-associated cytoskeleton in rat liver sinusoidal endothelial cells. Hepatology 21:180–189.

Braet F, Kalle WHJ, De Zanger RB, de Grooth BG, Raap AK, Tanke HJ, Wisse E. 1996. Comparative atomic force and scanning electron microscopy: An investigation on fenestrated endothelial cells in vitro. J Microsc 181:10–17.

Braet F, De Zanger R, Wisse E. 1997a. Drying cells for SEM, AFM and TEM by hexamethyldisilazane: A study on hepatic endothelial cells. J Microsc 186:84–87.

Braet F, De Zanger R, Kämmer S, Wisse E. 1997b. Noncontact versus contact imaging: An atomic force microscopic study on hepatic endothelial cells in vitro. Int J Imag Syst Technol 8:162–167.

Braet F, Rotsch C, Wisse E, Radmacher M. 1998a. Comparison of fixed and living liver endothelial cells by atomic force microscopy. Appl Phys A 66:S575–S578.

Braet F, Spector I, De Zanger R, Wisse E. 1998b. A novel structure involved in the formation of liver endothelial cell fenestrae revealed using the actin inhibitor misakinolide. Proc Natl Acad Sci USA 95: 13635–13640.

Braet F, De Zanger R, Seynaeve C, Baekeland M, Wisse E. 2001a. A comparative atomic force microscopy study on living skin fibroblasts and liver endothelial cells. J Electron Microsc 50:283–290.

Braet F, Luo D, Spector I, Vermijlen D, Wisse E. 2001b. Endothelial and pit cells. In: Arias I, Boyer JL, Fausto N, Jakoby WB, Schachter DA, Schafritz DA, editors. The liver: Biology and pathobiology, 4th ed. New York: Raven Press, pp. 437–453.

Braet F, Spector I, Shochet NR, Crews P, Higa T, Menu E, De Zanger R, Wisse E. 2002b. The new anti-actin agent dihydrohalichondramide reveals fenestrae-forming centers in hepatic endothelial cells. BMC Cell Biol 3:7.

Braet F, Bomans PHH, Wisse E, Frederik PM. 2003a. The observation of intact hepatic endothelial cells by cryo-electron microscopy. J Microsc 212:175–185.

Braet F, Muller M, Vekemans K, Wisse E, Le Couteur D. 2003b. Antimycin A-induced defenestration in rat hepatic sinusoidal endothelial cells. Hepatology 38:394–402.

Carrington WA, Lisin D. 2004. Cluster computing for digital microscopy. Microsc Res Tech 64:204–213.

Frank J, Wagenknecht T, McEwen BF, Marko M, Hsieh CE, Mannella CA. 2002. Three-dimensional imaging of biological complexity. J Struct Biol 138:85–91.

Fraser R, Dobbs BR, Rogers GWT. 1995. Lipoproteins and the liver sieve: The role of the fenestrated sinusoidal endothelium in lipoprotein metabolism, atherosclerosis, and cirrhosis. Hepatology 21:863–874.

Frederik PM, Hubert DH. 2005. Cryo electron microscopy of liposomes. Methods Enzymol 391;431–448.

Frederik PM, Stuart MC, Bomans PH, Busing WM, Burger KN, Verkleij AJ. 1991a. Perspective and limitations of cryo-electron microscopy—From model systems to biological specimens. J Microsc 161: 253–262.

Frederik PM, Bomans PH, Stuart MC. 1991b. The ultrastructure of cryo-sections and intact vitrified cells the effects of cryoprotectants and acceleration voltage on beam induced bubbling. Scan Microsc 5:S43–S51.

Frederik PM, Bomans PHH, Braet F, Wisse E. 1997. Cryo-electron microscopy of cultured hepatic endothelial cells. In: Wisse E, Knook DL, Balabaud C, editors. Cells of the hepatic sinusoid 6. Leiden: Kupffer Cell Foundation. pp. 476–478.

Frederik P, Bomans P, Franssen V, Laeven P. 2000. A vitrification robot for time resolved cryo-electron microscopy. In: Čech S, Janisch R, editors. Proceedings of the 12th European congress on electron microscopy, Vol. I. Brno: Reklamní Atelier Kupa. pp. B383–B384.

Geerts WJC, Koster AJ, Verkleij AJ, Humbel BM. 2006. Electron microscopy tomography and localization of proteins and macromolecular complexes in cells. In: Golemis E, Adams P, editors. Protein-protein interactions: A molecular cloning manual, 2nd ed. Cold Spring Harbor: Cold Spring Harbor Laboratory Press. pp. 715–739.

Grabenbauer M, Geerts WJC, Fernadez-Rodriguez J, Hoenger A, Koster AJ, Nilsson T. 2005. Correlative microscopy and electron tomography of GFP through photooxidation. Nat Methods 2:857–862.

Grunewald K, Medalia O, Gross A, Steven AC, Baumeister W. 2003. Prospects of electron cryotomography to visualize macromolecular complexes inside cellular compartments: Implications of crowding. Biophys Chem 100:577–591.

Kassies R, Van Der Werf KO, Lenferink A, Hunter CN, Olsen JD, Subramaniam V, Otto C. 2005. Combined AFM and confocal fluorescence microscope for applications in bio-nanotechnology. J Microsc 217:109–116.

King MV. 1991. Dimensional changes in cells and tissues during specimen preparation for the electron microscope. Cell Biophys 18:31–55.

Koster AJ, Klumperman J. 2003. Electron microscopy in cell biology: Integrating structure and function. Nat Rev Mol Cell Biol Sep:S6–S10.

Leapman RD. 2004. Novel techniques in electron microscopy. Curr Opin Neurobiol 14:591–598.

Lievens J, Snoeys J, Vekemans K, Van Linthout S, De Zanger R, Collen D, Wisse E, De Geest B. 2004. The size of sinusoidal fenestrae is a critical determinant of hepatocyte transduction after adenoviral gene transfer. Gene Ther 11:1523–1531.

Lillehei PT, Bottomley LA. 2000. Scanning probe microscopy. Anal Chem 72:189R–196R.

Lindroth M, Bell PB, Fredriksson BA, Xiao-Dong L. 1992. Preservation and visualisation of molecular structure in detergent-extracted whole mounts of cultured cells. Microsc Res Tech 22:130–150.

Mastronarde DN. 1997. Dual-axis tomography: An approach with alignment methods that preserve resolution. J Struct Biol 120:343–352.

McEwen BF, Frank J. 2001. Electron tomographic and other approaches for imaging molecular machines. Curr Opin Neurobiol 11:594–600.

Mironov AA, Polishchuk RS, Luini A. 2000. Visualizing membrane traffic in vivo by combined video fluorescence and 3D electron microscopy. Trends Cell Biol 8:349–353.

Peachey LD, Ishikawa H, Murakami T. 1996. Correlated confocal and intermediate voltage electron microscopy imaging of the same cells using sequential fluorescence labeling, fixation, and critical point dehydration. Scan Microsc 10:237–247.

Penczek P, Marko M, Buttle K, Frank J. 1995. Double-tilt electron tomography. Ultramicroscopy 60:393–410.

Radmacher M. 2002. Measuring the elastic properties of living cells by the atomic force microscope. Methods Cell Biol 68:67–90.

Robinson JM. 2001a. Biological labeling and correlative microscopy. Acta Histochem 103:261–264.

Robinson JM, Takizawa T, Pombo A, Cook PR. 2001b. Correlative fluorescence and electron microscopy on ultrathin cryosections: Bridging the resolution gap. J Histochem Cytochem 49:803–808.

Svitkina TM, Borisy GG. 1999. Arp2/3 complex and actin depolymerizing factor/cofilin in dendritic organization and treadmilling of actin filament array in lamellipodia. J Cell Biol 45:1009–1026.

Takizawa T, Robinson JM. 2003. Ultrathin cryosections: An important tool for immunofluorescence and correlative microscopy. J Histochem Cytochem 51:707–714.

Takizawa T, Robinson JM. 2006. Correlative microscopy of ultrathin cryosections in placental research. Methods Mol Med 121:351–369.

Taylor KA, Reedy MC, Cordova L, Reedy MK. 1984. Three-dimensional reconstruction of rigor insect flight muscle from tilted thin sections. Nature 310:285–291.

Templeton NS, Lasic DD, Frederik PM, Strey HH, Roberts DD, Pavlakis GN. 1997. Improved DNA: Liposome complexes for increased systemic delivery and gene expression. Nat Biotechnol 15:647–652.

Tsien RY. 2003. Imagining imaging's future. Nat Rev Mol Cell Biol Sep:S16–S21.

Wisse E. 1970. An electron microscopic study of the fenestraeted endothelial lining of rat liver sinusoids. J Ultrastruct Res 31:125–150.

Wisse E. 1972. An ultrastructural characterization of the endothelial cell in the rat liver sinusoid under normal and various experimental conditions, as a contribution to the distinction between endothelial and Kupffer cells. J Ultrastruct Res 38:528–562.

Wisse E, De Zanger RB, Charels K, Van Der Smissen P, McCuskey RS. 1985. The liver sieve: Considerations concerning the structure and function of endothelial fenestrae, the sinusoidal wall and the space of Disse. Hepatology 5:683–692.